
SUPERMESHING: A NOVEL METHOD FOR BOOSTING THE MESH DENSITY IN NUMERICAL COMPUTATION WITHIN 2D DOMAIN

Handing Xu^{1,3} Zhenguo Nie^{1,2,*} Qingfeng Xu^{1,4} Xinjun Liu^{1,2,*}

¹The State Key Laboratory of Tribology &

Tsinghua University (DME)-Siemens Joint Research Center for Advanced Robotics,
Department of Mechanical Engineering (DME), Tsinghua University, Beijing 100084, China

²Beijing Key Lab of Precision/Ultra-precision Manufacturing Equipments and Control,
Tsinghua University, Beijing 100084, China

³School of Mechatronical Engineering, Beijing Institute of Technology, Beijing 100084, China

⁴School of Computing and Information Systems, Melbourne School of Engineering,
University of Melbourne, Melbourne 3000, Australia

April 5, 2021

ABSTRACT

Due to the limit of mesh density, the improvement of the spatial precision of numerical computation always leads to a decrease in computing efficiency. Aiming at this inability of numerical computation, we propose a novel method for boosting the mesh density in numerical computation within 2D domain. Based on the low mesh-density stress field in 2D plane strain problem computed by the finite element method, this method utilizes a deep neural network named SuperMeshingNet to learn the non-linear mapping from low mesh-density to high mesh-density stress field, and realizes the improvement of numerical computation accuracy and efficiency simultaneously. We adopt residual dense blocks to our mesh-density boost model – SuperMeshingNet for extracting abundant local features and enhancing the prediction capacity of the model. Experimental results show that the SuperMeshingNet proposed in this work can effectively boost the spatial resolution of the stress field under the multiple scaling factors: $2\times$, $4\times$, $8\times$. Compared to the results of finite element method, the predicted stress field error of SuperMeshingNet is only 0.54%, which is within the acceptable range of stress field estimation, and the SuperMeshingNet predicts the maximum stress value also without significant accuracy loss. We publicly share our work with full detail of implementation at https://github.com/zhenguonie/2021_SuperMeshing_2D_Plane_Strain.

1 Introduction

Numerical computation, especially the finite element analysis (FEA) is widely used in various fields of scientific research[1, 2], especially in mechanical fields such as structural performance evaluation[3] and topology optimization[4]. Essentially, FEA is a kind of computer technology, which discretizes the continuous physical system and solves this discretization model. Because it determines the fineness of the continuous system discretization, mesh density is an important factor in FEA. At the same time, the computing cost of solving the discretized linear equations is linearly proportional to the mesh density. This relation results in the impossibility of improving the spatial resolution and computing efficiency of FEA simultaneously.

In view of the low computational efficiency of FEA under high mesh density, two kinds of solutions were proposed in recent years: adaptive mesh refinement (AMR), machine-learning based physical field prediction. AMR uses coarser mesh in unimportant area, and finer mesh in the interesting area, so as to obtain a better solution with less mesh. Berger

*Address all correspondences to these authors (zhenguonie@tsinghua.edu.cn).

et al.[5] first proposed an algorithm based on recursive iteration to achieve the local mesh density increase. After that, more research[6, 7, 8, 9] was performed to propose various enhanced AMR algorithms on this basis, and plenty of open source libraries were established[10, 11]. However, the AMR algorithms still require multiple iterations to gradually decide which part needs a finer mesh and obtain higher numerical accuracy. The increase in spatial resolution is still accompanied by the decrease in computing efficiency. The AMR algorithm cannot fundamentally solve the contradiction between the spatial resolution and the computing efficiency of FEA.

Machine-learning based methods can predict the physical field in one-shot getting rid of the iterative process, using the data-driven framework to map from input physical conditions to output physical fields. Liang et al.[12] first proposed a groundbreaking stress field estimation method based on deep learning. Their work concentrated on the stress field of the human thoracic aorta. The trained model can output the stress field of the thoracic aorta within one second after inputting the shape of the aorta. This method has significantly improved the efficiency, but only suitable for the estimation of the stress field of the thoracic aorta. Bhatnagar et al.[13] proposed an approximation model based on a convolutional neural network (CNN) for flow field predictions. Compared with the finite element method (FEM), the efficiency of this model is improved by 1-2 orders of magnitude. These progress proves the potential of machine learning in solving the contradiction between spatial resolution and computing efficiency. However, numerous training data are needed for these models and limit the prediction on prior unseen cases.

In our work, we proposed a novel method for boosting the mesh density in physical field prediction within 2D domain. Our method considers the mesh density in the numerical computing field to the image resolution in the image super-resolution field. This image-based problem representation allows the analysis of arbitrary 2D planar structures. We propose the SuperMeshingNet, which focuses on the 2D plane strain problem. SuperMeshingNet inputs low mesh-density stress field computed by FEM, takes high mesh-density physical field as the target, and outputs the generated high mesh-density physical field (Figure 1 shows a pair of low mesh-density and high mesh-density stress field). Predicting the stress field by SuperMeshingNet, less computing resources are needed on high mesh density compared to FEM, thereby fairly avoiding the conflict between the spatial resolution and the computing efficiency of FEA. In our test, we generate a dataset containing 3240 different boundary and load conditions. Under the mesh-density scaling factor is 8, the average relative stress error is only 0.54%, and the average computing speed is increased by 13.36 times than FEM.

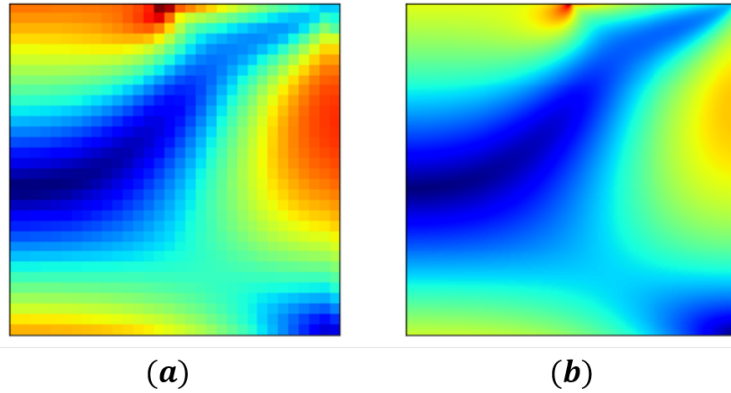


Figure 1: Low mesh-density (32×32) stress field (a) and High mesh-density (256×256) stress field (b).

2 Related Work

Our review focuses on studies that highlight physical field prediction based on deep learning, image super resolution, and two neural network architectures closely related to our work.

2.1 Physical Field Prediction Based on Deep Learning

Lots of research[12, 14] have proved that machine learning has excellent application potential and prospects in the field of physical field prediction. Ladický et al.[15] proposed a regression forest-based fluid simulation method for the prediction of the flow field. Compared with FEM, the computational efficiency of this model is improved by 1-3 orders of magnitude, which has a good alternative potential of the traditional method. Bhatnagar et al.[13] proposed a flow field prediction model based on CNN. In the research of Nie et al., CNN and GAN have been used for structural

analysis[16, 17] and topology optimization[18]. Besides, a physical field predicts method based on GNN had been proposed in the research of Pfaff et al.[14], this model can widely apply to the dynamic simulation of various physical systems. Compared with FEM, all of the deep learning based studies have greatly improved the computing efficiency.

Compared with machine learning completely replacing finite element analysis, another idea of combining machine learning with numerical computing has attracted more and more attention in recent years. Xie et al.[19] proposed a super-resolution model of flow field based on a generative adversarial network (GAN) - tempoGAN, the model can output clearer four-dimensional (x, y, z and t) flow field by inputting the flow field obtained by FEM. Belbute et al.[20] combined GNN and partial differential equation (PDE) solution, proposed a flow field prediction method, calculate low mesh-density flow field by PDE, then input it with high density mesh into GNN, output the high mesh-density flow field. Although both methods obtain flow field results with high accuracy and high computing efficiency, there are still issues with versatility.

2.2 Image Super Resolution

Image super resolution solves the problem of HD reconstruction of low resolution images, which requires to recover natural and clear textures from low resolution images, and finally obtains high resolution images. In recent years, supervised neural networks have become the most advanced technology in the field of image super resolution. The SRCNN proposed by Dong et al.[21] applied CNN to image super resolution field for the first time. Shi et al.[22] proposed a sub-pixel convolutional layer instead of pre-upsampling in the ESPCN model, this architecture not only achieves better SR effect, but also has a great advantage in speed. Lim et al.[23] proved the MAE loss function is better than MSE in the field of image super resolution in their work. The VDSR model proposed by Kim et al.[24] and the SRDenseNet model proposed by Tong et al.[25] first introduced residual learning and dense block to image super resolution separately, both of these work bring great contributions to the image super-resolution field. On the basis of these models, researchers in this field have developed a variety of super resolution models[26, 27, 28, 29].

Compare the mesh density increase of stress field and the super resolution of image, it's easy to find out that they are very similar. Therefore, using image processing methods to process the physical field is of great significance both in theory and practice.

2.3 Residual Learning and Residual Dense Block

The increase in the depth of the neural network will not only improve the non-linear expressiveness, it will also bring about problems such as network degradation. He et al.[30] proposed residual learning in order to solve this problem, the architecture is shown in Figure 2. For a stacked convolutional layer model, the input is x , assume the feature to be learned is $H(x)$, then we let the model learn its residual $F(x) = H(x) - x$ rather than itself $H(x)$. Intuitively, because the residuals to be learned are generally smaller than original feature, there is less content to learn, result in the learning difficulty decrease.

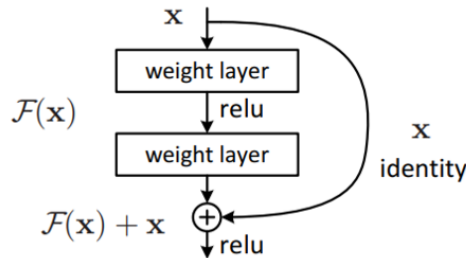


Figure 2: Residual learning architecture.[30]

Zhang et al.[26] proposed residual dense block (RDB) in RDN, this architecture integrates dense connection layer, local feature fusion and local residual learning. As shown in Figure 3 and Equation (1), it synthetically uses the features of $F_{d-1}, F_{d,c}$ and forms a continuous memory mechanism, thus can more effectively use the feature information of the image and enhance the expressive ability of the model.

$$\begin{aligned}
F_d &= F_{d-1} + F_{d,LF} \\
F_{d,LF} &= H_{LFF}^d([F_{d-1}, F_{d,1}, \dots, F_{d,c}, \dots, F_{d,C}]) \\
F_{d,c} &= \sigma(W_{d,c}[F_{d-1}, F_{d,1}, \dots, F_{d,c-1}])
\end{aligned} \tag{1}$$

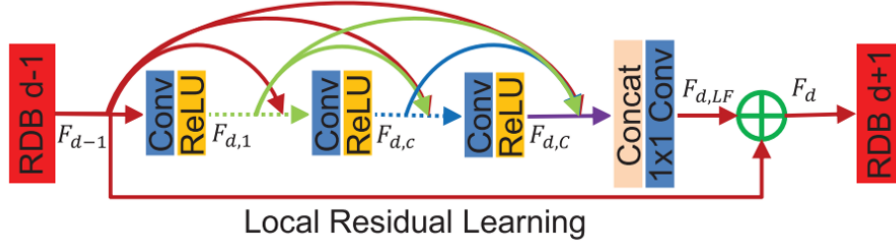


Figure 3: Residual dense block (RDB) architecture.[26]

where H_{LF}^d denotes the function of the 1×1 convolutional layer, σ denotes the ReLU activation function and $W_{d,c}$ denotes the weights of the c -th convolutional layer.

2.4 Sub-pixel Convolution Layer

The sub-pixel convolution layer is proposed for upsampling in ESPCN by Shi et al.[22] The layer architecture is shown in Figure 4. Assuming that the size of the low resolution image is $x \times y \times c$, the scale is r , the size of feature map T learned in the penultimate layer of the model is $x \times y \times r^2 c$. In sub-pixel convolution layer, rearranges the $r^2 c$ channels to the size of $rx \times ry \times c$, the rearrangement rules are shown in Equation (2):

$$PS(T)_{x,y,c} = T_{\lfloor x/r \rfloor, \lfloor y/r \rfloor, c \cdot r \cdot \text{mod}(y,r) + c \cdot \text{mod}(x,r)} \quad (2)$$

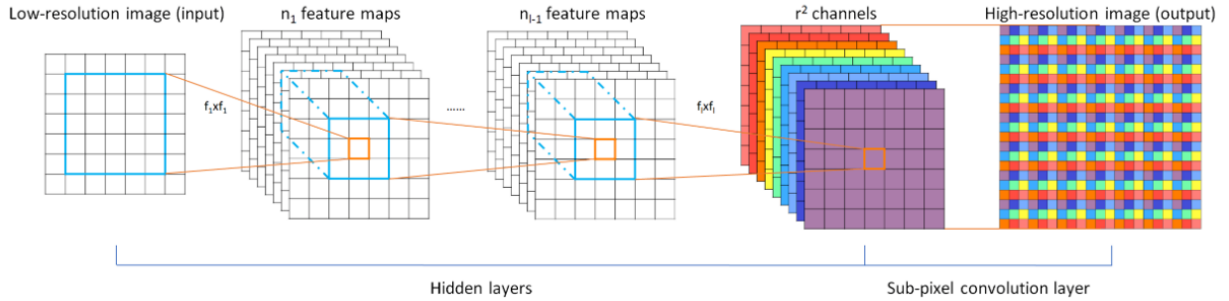


Figure 4: The structure of ESPCN, the last two layers make up the sub-pixel convolution layer.[22]

Though this layer architecture is called sub-pixel convolutional layer, it actually does not perform the convolution operation. It's an efficient and parameter-free pixel rearrangement method. Therefore, it greatly improves the study speed of the entire model. On the other hand, because of this architecture, the model is upsampled at the end, so that the model can retain more texture information in the low resolution space and improve the reconstruction effect.

3 Technical Approach

This work proposes a method for boosting the mesh density in physical field prediction within 2D domain. We calculate the stress field of 2D plane structure with linear isotropic elastic material. The approach takes the structure geometry, external loads, displacement boundary conditions and low density mesh as the input of FEM, and the low mesh-density von-mises stress field obtained is used as the input of the neural network to output the high mesh-density von-mises stress field. Based on this method, we propose a neural network architecture — SuperMeshingNet.

3.1 Problem Description

Consider the structure shown in Figure 5 is composed of a homogeneous and isotropic linear elastic material. We treat this structure as a plane strain problem. The load is applied to the upper boundary of the structure, and different types of

displacement boundary conditions are applied to other boundaries. The evenly distributed external force q is applied in both the horizontal and vertical directions. The magnitudes of the two components denoted by q_x and q_y vary separately within a prescribed window of magnitude. The displacement boundary conditions includes completely fixed, horizontal constraint, vertical constraint and so on. The material properties are kept unchanged for all samples.

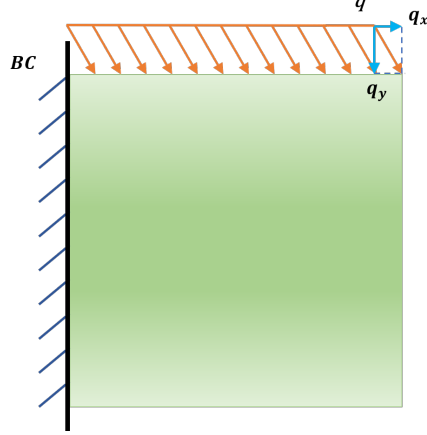


Figure 5: A sample of a plane strain problem with linear isotropic material. BC denotes the boundary condition, q denotes the external force.

The constitutive equation of the plane strain problem consist of the geometric equation (3), equilibrium equation (4) and physical equation, the generalized Hooke law (5):

$$\varepsilon_{ij} = \frac{1}{2}(u_{i,j} + u_{j,i}) \quad (3)$$

$$\sigma_{ij,j} + f_i = 0 \quad (4)$$

$$\begin{bmatrix} \sigma_{xx} \\ \sigma_{yy} \\ \sigma_{xy} \end{bmatrix} = \frac{E}{(1-2\mu)(1+\mu)} \begin{bmatrix} 1-\mu & \mu & 0 \\ \mu & 1-\mu & 0 \\ 0 & 0 & \frac{1-2\mu}{2} \end{bmatrix} \begin{bmatrix} \varepsilon_{xx} \\ \varepsilon_{yy} \\ \varepsilon_{xy} \end{bmatrix} \quad (5)$$

where all equations are expressed in Einstein notation, i and j subscripts with value of 1 or 2, u_i denotes the displacement in x_i axis, σ_{ij} and ε_{ij} denotes the stress and strain on surface x_i in x_j direction respectively, f_i denotes the body force component in x_i direction, E denotes the Young's Modules, and μ denotes the Poisson's ratio.

3.2 Dataset Generation

We use the commercial FEA software ANSYS to generate the dataset required for SuperMeshingNet training and testing. The element node type is 4-node quadrilateral. Figure 6 shows randomly selected samples from a total of 3240 samples.

Each sample is composed of 4 images with different resolutions, which represent the von-mises stress field calculated by FEM with four mesh densities 24×24 , 48×48 , 128×128 and 256×256 from left to right. The neural network model inputs the stress field results of the 24×24 mesh density, and uses the stress field results of other mesh densities as ground truth. Among all samples, the von-mises stress varies from 0 to 227.8MPa with an average of 3.53MPa.

Besides, in our experiments, we randomly rotate all samples during training to increase the diversity of the load and boundary conditions, improve the predictive ability of the model to deal with more input conditions.

3.3 SuperMeshingNet Architecture

As shown in Figure 7, the proposed SuperMeshingNet increases the mesh density of the von-mises stress field. Model inputs low mesh-density stress field and outputs high mesh-density stress field, where each pixel represents the von-mises stress.

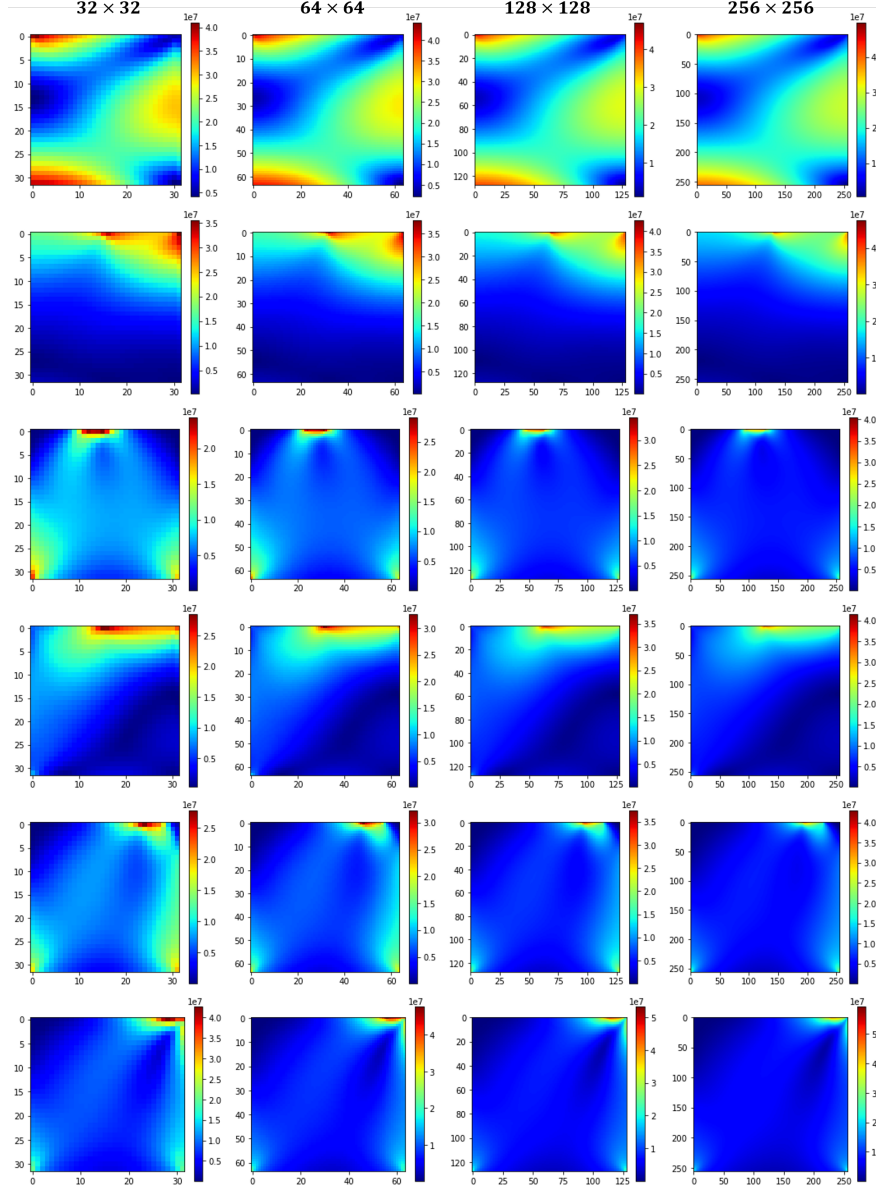


Figure 6: Dataset samples calculated by FEM. The mesh density from left to right is 32×32 , 64×64 , 128×128 and 256×256 .

For SuperMeshingNet, we use the two convolutional layers C_1 and C_2 to extract the shallow feature of the input stress field image. Because of the similarity between the low and high mesh-density stress field, a global residual learning structure is introduced after C_1 , so that the network can concentrate on the high-frequency information of the stress field to get better result.

After extracting the shallow feature, we utilize multiple RDBs for deep feature extraction. The deep feature in the low mesh-density stress field is extracted by cascading multiple RDBs. Then, concatenate the feature map extracted from each RDB and input into C_3 . The feature extracted from each RDB can be further comprehensively used because of the concatenation. Convolutional layer C_3 has a filter with a kernel of 1×1 , which is introduced to reduce the feature map dimension to reduce the network training difficulty.

Finally, we adopt a sub-pixel convolutional layer SP for upsampling. Through the rearrangement of multiple feature maps, increase the scale of the feature map and obtain the stress field image with increased mesh density.

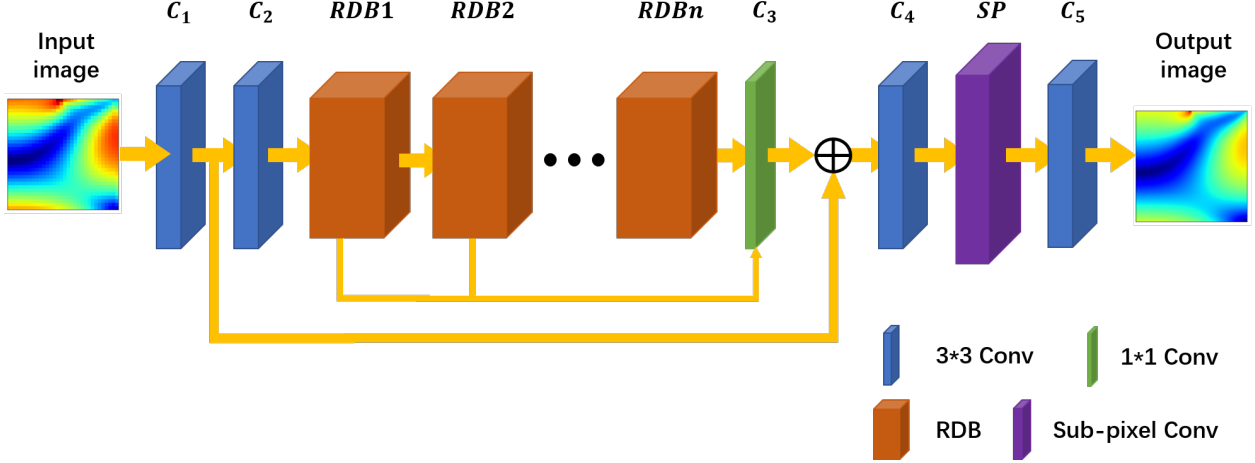


Figure 7: The architecture of SuperMeshingNet.

In our approach, each convolutional layer has 64 filters, and the kernel size of all filters is 3×3 except filters in C_3 , which is 1×1 .

3.4 Loss Function and Metrics

In our work, we select mean absolute error (MAE) as the loss function of our model for training. The predicted result of model $\hat{\sigma}$ and ground truth σ are represented by image, according to different mesh-density scaling factor, the resolutions of the images are 64×64 , 128×128 and 256×256 respectively. $\hat{\sigma}$ and σ are reshaped into 1D vector before calculating MAE, $\hat{\sigma}$ is represented by $\hat{\sigma} = \{\hat{\sigma}_1, \hat{\sigma}_2, \dots, \hat{\sigma}_n\}$, and σ is represented by $\sigma = \{\sigma_1, \sigma_2, \dots, \sigma_n\}$, MAE is:

$$MAE = \frac{1}{n} \sum_{i=1}^n |\hat{\sigma}_i - \sigma_i| \quad (6)$$

where n is the amount of image pixels.

4 Result and Discussion

Our SuperMeshingNet is implemented by Pytorch, trained and tested on Nvidia GeForce GTX 2080Ti GPU. We carry out the following experiments and analyze the results to verify the feasibility of our method. First, we compare SuperMeshingNet with FEM in the case of mesh-density scaling factor is 8, which prove the superiority of our method. Second, we test the effect of the number of different RDBs D and the number of convolutional layers C in them. Then, we analyze the effect of SuperMeshingNet on different mesh-density scaling factor. Finally, we test the effect of the model for the prediction of maximum stress.

4.1 Accuracy and Performance

In our experiments, we train and evaluate our SuperMeshingNet using the whole dataset. The training data size is 3000, and the test data size is 240. Figure 8 shows several test results under mesh-density scaling factor is 8, the images from left to right are the input low mesh-density stress field, the input high mesh-density stress field, the generated high mesh-density stress field and the difference of the generated stress field and the ground truth separately. The average relative stress error (ARSE, defined as Equation (7)) between the generated high mesh-density stress field and the ground truth is only 0.54%, which we deem is within the acceptable range of stress field estimation.

$$ARSE = \frac{1}{nm} \sum_{i=1}^n \sum_{j=1}^m \left| \frac{\hat{\sigma}_i(j) - \sigma_i(j)}{\sigma_i(j)} \right| \quad (7)$$

where n denotes the amount of test cases, m denotes the amount of image pixels. $\hat{\sigma}_i(j)$, $\sigma_i(j)$ are the j th stress value of the i th test case of the generated high mesh-density stress field and the ground truth separately.

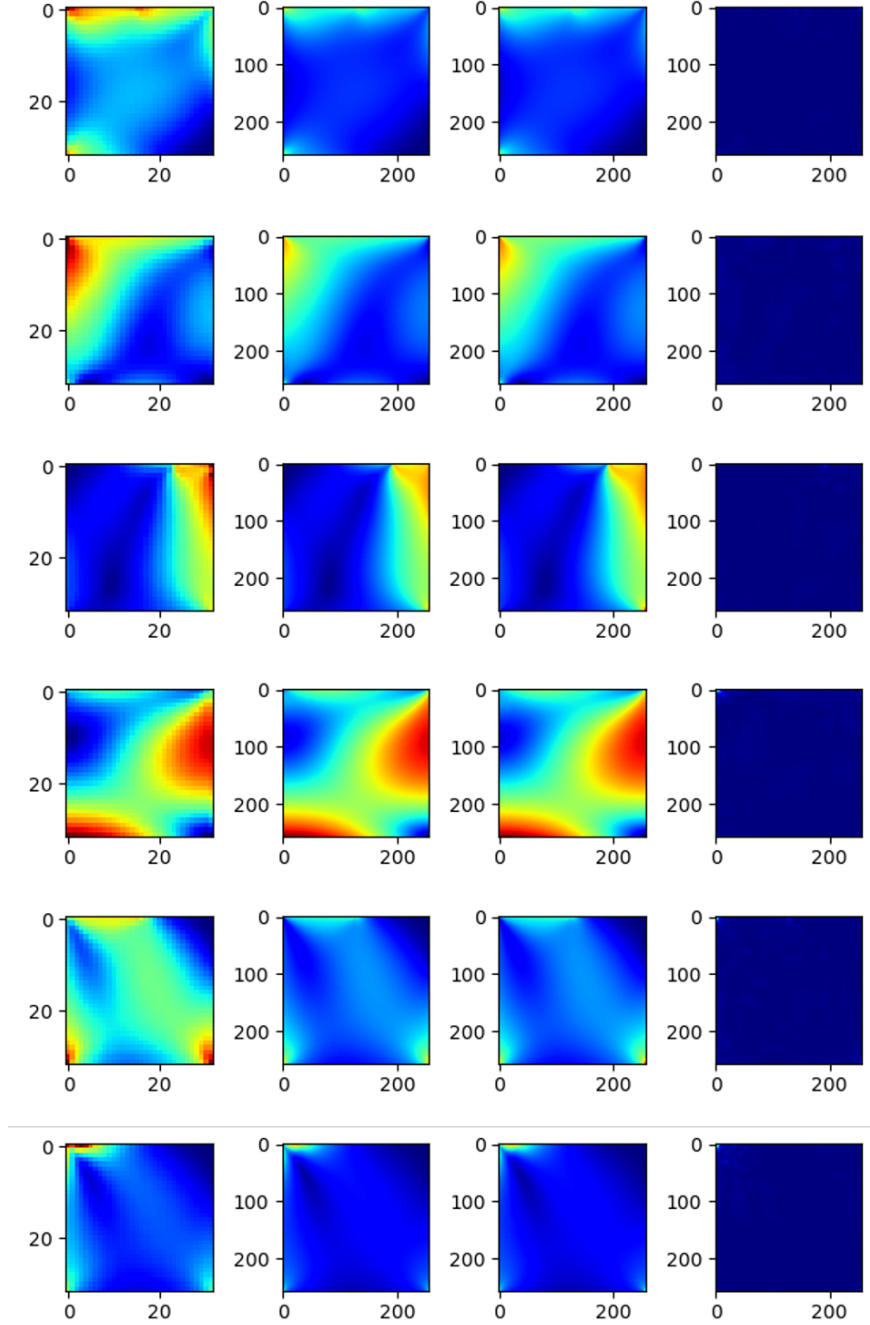


Figure 8: Several test results. the resolution of input image is 32×32 , output image is 256×256 .

In order to verify the efficiency of our method, we test the computing efficiency between our method and FEM. Under mesh-density scaling factor is 8, processing one sample by SuperMeshingNet in our method takes $0.715s$, and directly calculate high mesh-density stress field will cost $9.553s$. Our method is 13.36 times faster than FEM at the same mesh density. All finite element computation is accomplished by commercial FEA software ANSYS (on Intel i5-7200U CPU).

4.2 Effect of RDB Number and Number of Convolutional Layers per RDB

In order to obtain the best prediction performance, we test the effect of RDB number D and number of convolutional layers per RDB C through a series of experiments. We test a total of 6 experiments, in which $D = 8, 12, 16$ and $C = 4, 8$ separately. Figure 9 shows the MAE loss of these conditions under mesh-density scaling factor is 8. Comparing the three pairs of MAE loss at the same D value: $D16C8 - D16C4$, $D12C8 - D12C4$, $D8C8 - D8C4$, the performance of SuperMeshingNet is significantly getting better with the increase of C . But the MAE loss of SuperMeshingNet at $D16C8$, $D12C8$, $D8C8$ are almost the same, which means D has a slight effect on the model’s performance. This result is different from the conclusion in [26], which is larger D and C will lead to higher performance. We consider the reason to be SuperMeshingNet with smaller D can perform well on this problem, so blindly increase D will not further improve the performance. In our other experiments, we set $D = 8$ and $C = 8$ for satisfying performance and efficient training.

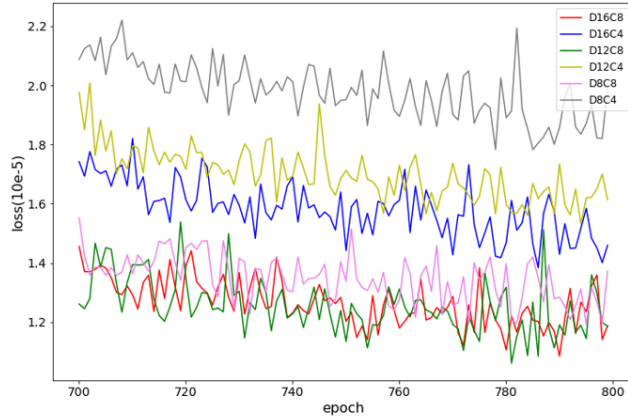


Figure 9: The MAE loss of different D (8, 12, 16) and C (4, 8) values in the last 100 epochs under 8 mesh-density scaling factor.

4.3 Effect on Different Mesh-density Scaling Factor

For the purpose of test the effect of our method under multiple mesh-density scaling factor 2, 4, 8, we respectively calculated the ARSE between the generated high mesh-density stress field and the ground truth, as shown in Table 1. All the ARSE are in the acceptable range under different mesh-density scaling factor, which indicates our SuperMeshingNet has excellent prediction performance under multiple mesh-density scaling factor.

Mesh density	64×64	128×128	256×256
ARSE	0.553%	0.547%	0.543%

Table 1: The ARSE compared with the result calculated by FEM.

We also test the computing efficiency of our method, the computing time comparison of our method and FEM is shown in Table 2. We can find that the computing efficiency hardly decrease with the increase of mesh-density scaling factor, because the mapping from low mesh-density stress field to high mesh-density stress field has low time complexity relatively, and the computation of low mesh-density stress field is mainly time-consuming. Compared with the decrease of FEM, it shows that our method is more competitive in the computation of stress field with high mesh density.

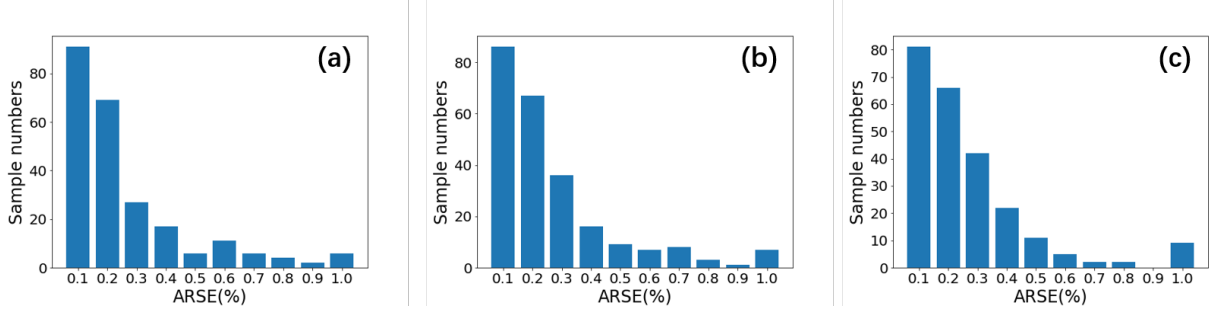
4.4 Prediction of Maximum Stress

For most plane strain problems, we mainly concerned about the maximum stress and its location to determine whether failure will occur at somewhere, so we test the prediction performance of maximum stress by our SuperMeshingNet. Figure 10 shows the distribution of the maximum stress difference between generated high mesh-density stress field and ground truth on different mesh-density scaling factor. It’s excellent that most of the maximum stress difference are

Mesh density	64×64	128×128	256×256
FEM+SuperMeshingNet	0.650	0.676	0.715
FEM	1.132	3.176	9.553

Table 2: The computing time comparison of our method and FEM.

under 0.4%, which proves the satisfying effect of SuperMeshingNet. However, we find that several cases' maximum difference is greater than 1.0%. We speculate the immature structure of SuperMeshingNet causes this, and we will continue to solve this problem in our future work.

Figure 10: The distribution of the maximum stress difference between SuperMeshingNet predict result and FEM computing result. (a): 64×64 , (b): 128×128 , (c): 256×256 .

5 Conclusions

In this work, we present a novel method for boosting the mesh density in physical field prediction within 2D domain. In plane strain problems, we propose a new convolutional neural network called SuperMeshingNet mapping from low mesh-density stress field to high mesh-density stress field. In addition, we generate the training and testing dataset, which contains 3240 samples of 32×32 , 64×64 , 128×128 , 256×256 mesh-density stress fields.

For the contradiction between spatial resolution and computing efficiency of FEA, we prove that our method can effectively predict physical field under various mesh densities through experiments. Compared to FEM, our method improve the computing efficiency 13.36 times faster than FEM under the same spatial resolution, and the average relative stress error is only 0.54%, which means the computing accuracy is kept within the acceptable range of stress field prediction.

In future work, we will focus on the unstructured mesh of the physical field relative to the image. Now we only take the structured mesh into consideration using CNN. Thus, it is more valuable that processing the more commonly used unstructured mesh by GNN. Moreover, integrating the inherent characteristics of the physical field (the strain continuity of the stress field, etc.) into neural network design can help improve prediction performance.

References

- [1] Jen A Bright and Emily J Rayfield. The response of cranial biomechanical finite element models to variations in mesh density. *The Anatomical Record: Advances in Integrative Anatomy and Evolutionary Biology*, 294(4):610–620, 2011.
- [2] Andri Afrizal, Syifaul Huzni, Sulaiman Thalib, HPS Abdul Khalil, Samsul Rizal, et al. Effect of mesh sensitivity and cohesive properties on simulation of typha fiber/epoxy microbond test. *Computation*, 8(1):2, 2020.
- [3] Chul Hun Chung, Jungwhee Lee, and Jong Ho Gil. Structural performance evaluation of a precast prefabricated bridge column under vehicle impact loading. *Structure and Infrastructure Engineering*, 10(6):777–791, 2014.
- [4] Jen A Bright and Emily J Rayfield. The response of cranial biomechanical finite element models to variations in mesh density. *The Anatomical Record: Advances in Integrative Anatomy and Evolutionary Biology*, 294(4):610–620, 2011.

- [5] Marsha J Berger and Joseph Oliger. Adaptive mesh refinement for hyperbolic partial differential equations. *Journal of computational Physics*, 53(3):484–512, 1984.
- [6] P Areias, J Reinoso, PP Camanho, J César De Sá, and Timon Rabczuk. Effective 2d and 3d crack propagation with local mesh refinement and the screened poisson equation. *Engineering Fracture Mechanics*, 189:339–360, 2018.
- [7] Carsten Burstedde, Lucas C Wilcox, and Omar Ghattas. p4est: Scalable algorithms for parallel adaptive mesh refinement on forests of octrees. *SIAM Journal on Scientific Computing*, 33(3):1103–1133, 2011.
- [8] Raphael Egan and Frédéric Gibou. Fast and scalable algorithms for constructing solvent-excluded surfaces of large biomolecules. *Journal of Computational Physics*, 374:91–120, 2018.
- [9] Igor Kossaczky. A recursive approach to local mesh refinement in two and three dimensions. *Journal of Computational and Applied Mathematics*, 55(3):275–288, 1994.
- [10] Peter MacNeice, Kevin M Olson, Clark Mobarry, Rosalinda De Fainchtein, and Charles Packer. Paramesh: A parallel adaptive mesh refinement community toolkit. *Computer physics communications*, 126(3):330–354, 2000.
- [11] Weiqun Zhang, Ann Almgren, Vince Beckner, John Bell, Johannes Blaschke, Cy Chan, Marcus Day, Brian Friesen, Kevin Gott, and Daniel Graves. Amrex: a framework for block-structured adaptive mesh refinement. *Journal of Open Source Software*, 4(37):1370–1370, 2019.
- [12] L. Liang, M. Liu, C. Martin, and W. Sun. A deep learning approach to estimate stress distribution: a fast and accurate surrogate of finite-element analysis. *J R Soc Interface*, 15(138), 2018.
- [13] Saakaar Bhatnagar, Yaser Afshar, Shaowu Pan, Karthik Duraisamy, and Shailendra Kaushik. Prediction of aerodynamic flow fields using convolutional neural networks. *Computational Mechanics*, 64(2):525–545, 2019.
- [14] Tobias Pfaff, Meire Fortunato, Alvaro Sanchez-Gonzalez, and Peter W Battaglia. Learning mesh-based simulation with graph networks. *arXiv preprint arXiv:2010.03409*, 2020.
- [15] L’ubor Ladický, SoHyeon Jeong, Barbara Solenthaler, Marc Pollefeys, and Markus Gross. Data-driven fluid simulations using regression forests. *ACM Transactions on Graphics (TOG)*, 34(6):1–9, 2015.
- [16] Zhenguo Nie, Haoliang Jiang, and Levent Burak Kara. Stress field prediction in cantilevered structures using convolutional neural networks. *Journal of Computing and Information Science in Engineering*, 20(1), 2020.
- [17] Haoliang Jiang, Zhenguo Nie, Roselyn Yeo, Amir Barati Farimani, and Levent Burak Kara. Stressgan: A generative deep learning model for two-dimensional stress distribution prediction. *Journal of Applied Mechanics*, 88(5):051005, 2021.
- [18] Zhenguo Nie, Tong Lin, Haoliang Jiang, and Levent Burak Kara. Topologygan: Topology optimization using generative adversarial networks based on physical fields over the initial domain. *Journal of Mechanical Design*, 143(3):031715, 2021.
- [19] You Xie, Erik Franz, Mengyu Chu, and Nils Thuerey. tempogan: A temporally coherent, volumetric gan for super-resolution fluid flow. *ACM Transactions on Graphics (TOG)*, 37(4):1–15, 2018.
- [20] Filipe de Avila Belbute-Peres, Thomas Economon, and Zico Kolter. Combining differentiable pde solvers and graph neural networks for fluid flow prediction. In *International Conference on Machine Learning*, pages 2402–2411. PMLR, 2020.
- [21] Chao Dong, Chen Change Loy, Kaiming He, and Xiaoou Tang. Learning a deep convolutional network for image super-resolution. In *European conference on computer vision*, pages 184–199. Springer, 2014.
- [22] Wenzhe Shi, Jose Caballero, Ferenc Huszár, Johannes Totz, Andrew P Aitken, Rob Bishop, Daniel Rueckert, and Zehan Wang. Real-time single image and video super-resolution using an efficient sub-pixel convolutional neural network. In *Proceedings of the IEEE conference on computer vision and pattern recognition*, pages 1874–1883, 2016.
- [23] Bee Lim, Sanghyun Son, Heewon Kim, Seungjun Nah, and Kyoung Mu Lee. Enhanced deep residual networks for single image super-resolution. In *Proceedings of the IEEE conference on computer vision and pattern recognition workshops*, pages 136–144, 2017.
- [24] Jiwon Kim, Jung Kwon Lee, and Kyoung Mu Lee. Deeply-recursive convolutional network for image super-resolution. In *Proceedings of the IEEE conference on computer vision and pattern recognition*, pages 1637–1645, 2016.
- [25] Tong Tong, Gen Li, Xiejie Liu, and Qinquan Gao. Image super-resolution using dense skip connections. In *Proceedings of the IEEE international conference on computer vision*, pages 4799–4807, 2017.

- [26] Yulun Zhang, Yapeng Tian, Yu Kong, Bineng Zhong, and Yun Fu. Residual dense network for image super-resolution. In *Proceedings of the IEEE conference on computer vision and pattern recognition*, pages 2472–2481, 2018.
- [27] Ying Tai, Jian Yang, Xiaoming Liu, and Chunyan Xu. Memnet: A persistent memory network for image restoration. In *Proceedings of the IEEE international conference on computer vision*, pages 4539–4547, 2017.
- [28] Yulun Zhang, Kunpeng Li, Kai Li, Lichen Wang, Bineng Zhong, and Yun Fu. Image super-resolution using very deep residual channel attention networks. In *Proceedings of the European conference on computer vision (ECCV)*, pages 286–301, 2018.
- [29] Xuecai Hu, Haoyuan Mu, Xiangyu Zhang, Zilei Wang, Tieniu Tan, and Jian Sun. Meta-sr: A magnification-arbitrary network for super-resolution. In *Proceedings of the IEEE/CVF Conference on Computer Vision and Pattern Recognition*, pages 1575–1584, 2019.
- [30] Kaiming He, Xiangyu Zhang, Shaoqing Ren, and Jian Sun. Deep residual learning for image recognition. In *Proceedings of the IEEE conference on computer vision and pattern recognition*, pages 770–778, 2016.